4. REENTRANT INDUCED SUPERCONDUCTIVITY IN HYBRID STRUCTURE WITH HIGH BARRIER TRANSPARENCY

E. Zubov[1, 2]

Abstract

Within the framework of the self-consistent effective field approximation of the time dependent perturbation theory, an influence of the electron tunneling on spontaneously induced order parameters in a hybrid structure «normal metal-superconductor» is considered. For a normal-metal model that does not take into account electron-electron scattering as well as electron-phonon coupling, it has been obtained a critical barrier transparency corresponding to the disappearance of superconductivity in the ground state. The presence of incoherent excitations leads to a complex relationship between the effects of ordering, thermal fluctuations, and tunneling. Near the critical barrier transparency, this can stabilize a superconducting state in the certain temperature regions. As a result, a reentrant superconductivity phenomenon is observed. The studied spectral properties of the hybrid structure reflect existence of both coherent and incoherent elementary excitations.

✉ Eduard Zubov
eezubov@ukr.net

[1] Kyiv Academic University, Vernadsky blvd. 36, 03142 Kyiv, Ukraine
[2] Vasyl' Stus Donetsk National University, 600-richchia vul. 21, 21021 Vinnytsia, Ukraine

4.1 Introduction

Despite a long history of the transport properties studies of the «normal metal-superconductor» hybrid structures, the problem of a rigorous quantum-mechanical consideration of proximity effect in such systems has not yet lost its relevance. This is especially evident in recent years in connection with the search and realization of Majorana fermions based on the proximity effect in the system of a superconductor with an s-symmetry gap and topological insulator with surface states [4.1]. This type of fermions is protected from decoherence and is of promising importance in the formation of qubit states for quantum computers. The problem of superconductivity as a quantum effect is rather complicated from the point of view of subsequent accounting for the correlation effects and influence of barriers in inhomogeneous structures. To date, to analyze a huge array of experimental data on electron tunneling, a wide range of theoretical methods for studying the observed phenomena in hybrid structures have been developed, which are based on the well-known equations of Gor'kov [4.2], Bogolyubov, P. de Gennes [4.3], McMillan [4.4] and their semiclassical approximations [4.5, 4.6]. It should be noted that in the study of critical temperatures, spectral and transport properties of hybrid structures consisting of a superconductor and normal magnetic or nonmagnetic metals, as a rule, a linear integral relationship is used for the coordinate dependence of the gap function using a nonlocal kernel [4.7–4.9]. However, in the case of sufficiently transparent barriers, when a perturbation in the form of tunnel Hamiltonian is significant, it is no longer possible to consider a linear approximation, since the contribution of electron correlations and scattering may turn out to be significant. In particular, the appearance of reentrant super-conductivity, found in the $Nb/Cu_{1-x}Ni_x$ bilayers [4.10], can be associated not only with the ferromagnetism of a normal metal but also with the effect of electron tunneling through a transparent barrier.

Earlier, we presented an effective field approximation in the framework of the diagrammatic method of perturbation theory for solving a wide range of problems in condensed matter physics [4.11]. In particular, in the zeroth approximation over an inverse effective radius of electron interactions, it is possible to build a quantum nonlinear theory of the proximity effect in a hybrid structure "normal metal-superconductor" with a tunnel barrier [4.12], in which

there are no the phenomenological parameters. Since electron-electron scattering is not taken into account in the Hamiltonian, this model corresponds to ballistic limit, when a mean free path is substantially greater than the film thickness. Such parameters of superconductivity as the coherence length or the penetration depth of superconducting correlations into a normal metal are derivatives of the theory and can be expressed in terms of the introduced microscopic parameters of the Hamiltonian and temperature.

The structure of the chapter is as follows. In Section 4.2, the tunneling Hamiltonian of the hybrid structure «normal metal-superconductor» (FMM-SC) with the main microscopic parameters of interactions is presented. The presence of ferromagnetism (FM) in the normal metal (N-metal) is also assumed. Further, the main goal of this work is to study the proximity effect for given model Hamiltonian, which is expressed in the site representation. It is possible if the Bloch electronic functions are replaced by localized Wannier functions for matrix elements. Thus, the unperturbed Hamiltonian with the energy of chemical potential allows us to easily average the arising correlators in any order of the time perturbation theory, and also to use graphical methods for summing diagrams in a wave space to determine the effective propagator lines. Section 4.3 gives a detailed calculation of the contributions to Green's functions taking into account the adiabatic switching on the interactions caused by the tunneling Hamiltonian, as well as the appearance of imaginary parts responsible for electron scattering, magnitude, and phase of the spontaneous order parameter. The results of numerical calculations of phase diagrams for the inverse proximity effect and spectral characteristics of SC are presented. In Section 4.4, it is studied an influence the tunnel SC electrons on order parameter, excitation spectrum, and spectral density of the FMM part in the hybrid structure. In Section 4.5, the main conclusions of the article are formulated.

4.2 Hamiltonian of the «normal metal-superconductor» electron system and the self- consistent order parameter

In a general case, the Hamiltonian for considered hybrid structure can be written as the sum of Hamiltonians $\hat{H}_N$, $\hat{H}_S$ for N-metal and SC, respectively, as well as the tunnel contribution $\hat{H}_T$:

$$\hat{H} = \hat{H}_N + \hat{H}_S + \hat{H}_T , \tag{4.1}$$

where for a N-metal in the site representation for the second quantized electron creation (annihilation) operators $c_{\sigma i}^+ (c_{\sigma i})$ with a spin σ

$$\hat{H}_N = \sum_{i,j,\sigma} t_{1ij} c_{\sigma i}^+ c_{\sigma j} - \sum_{i\sigma} \mu_\sigma c_{\sigma i}^+ c_{\sigma i} . \tag{4.2}$$

Here, t_{1ij} is the hopping integral, which determines the electron band energy, $\mu_\sigma = \mu_1 + \sigma J_0$, μ_1 is the chemical potential for N-metal, J_0 is the parameter of electron exchange interactions and $J_0 > 0$ for a ferromagnet. Also, $\sigma = \pm 1$ for saturated state and $\sigma = \pm 2 < \sigma_z >$ for magnet with a mean spin $< \sigma_z >$. For the superconducting part of this structure, we write in a general case the interaction Hamiltonian

$$\hat{H}_S = \sum_{i,j,\sigma} t_{2ij} a_{\sigma i}^+ a_{\sigma j} + \sum_{ij} \left(\sum_{\sigma\sigma'} V_{ij,ji}^C n_{i\sigma} n_{j\sigma'} - \sum_q \frac{\left| M_q \right|^2}{\omega_q} e^{iq(R_i - R_j)} n_i n_j \right) - \mu_2 \sum_{i\sigma} a_{\sigma i}^+ a_{\sigma i} , \tag{4.3}$$

where μ_2, t_{2ij} and $V_{ij,ji}^C$ are the SC chemical potential, electron band energy and energy of the Coulomb electron repulsion in the sites with occupancies $n_{i\sigma}$ and $n_{i\sigma'}$, $n_i = n_{i\sigma} + n_{i-\sigma}$, respectively. $\left| M_q \right|^2 / \omega_q$ is the constant of electron-phonon interaction [4.13] with phonon frequency ω_q and matrix element M_q. It is known that near the Fermi level with a width of the order of the Debye energy, the attraction of electrons prevails over their Coulomb repulsion [4.14]. Therefore, the second term in (4.3) can be written in the form:

$$\hat{H}_{El,-ph} = -\sum_{ij\sigma\sigma'} V_{ij}^{el.-ph} n_{i\sigma} n_{j\sigma'} \tag{4.4}$$

Spontaneous breaking of the Hamiltonian (4.4) symmetry is possible only in a fixed narrow energy area. Let us extract from (4.4) the order parameters corresponding to the superconducting phase in the form of anomalous correlators $< a_{i\sigma}^+ a_{j\sigma}^+ >$ and $< a_{j\sigma} a_{i\sigma} >$, where the symbol $<...>$ denotes the statistical averaging over the total Hamiltonian (4.1). For this, we write (4.4) as follows:

$$\hat{H}_{El.-ph} = -\sum_{ij\sigma\sigma'} V_{ij}^{el.-ph} a_{i\sigma}^+ a_{i\sigma} a_{j\sigma'}^+ a_{j\sigma'} = -\sum_{ij\sigma\sigma'} V_{ij}^{el.-ph} a_{i\sigma}^+ a_{j\sigma'}^+ a_{j\sigma'} a_{i\sigma} =$$
$$-\sum_{ij\sigma\sigma'} V_{ij}^{el.-ph} \left(\{ a_{i\sigma}^+ a_{j\sigma'}^+ - < a_{i\sigma}^+ a_{j\sigma'}^+ > \} + < a_{i\sigma}^+ a_{j\sigma'}^+ > \right) \left(\{ a_{j\sigma'} a_{i\sigma} - < a_{j\sigma'} a_{i\sigma} > \} + < a_{j\sigma'} a_{i\sigma} > \right). \tag{4.5}$$

The product of the terms in curly brackets describes the fluctuation effects of superconductivity, which are not considered here. Leaving only the operator terms in (4.5), we obtain the Hamiltonian in the molecular field approximation

$$\hat{H}_{El,-ph}^{MF} = -\sum_{ij\sigma} V_{ij}^{el.-ph} \left(a_{i\sigma}^+ a_{j-\sigma}^+ < a_{j-\sigma} a_{i\sigma} > + a_{j-\sigma} a_{i\sigma} < a_{i\sigma}^+ a_{j-\sigma}^+ > \right), \tag{4.6}$$

where $\sigma' = -\sigma$ for singlet Cooper pairing (s-superconductivity). Let us enter a gap function

$$\Delta_{ij\sigma} = V_{ij}^{el.-ph} < a_{j-\sigma} a_{i\sigma} >. \tag{4.7}$$

Then the Hamiltonian (4.7) takes the form:

$$\hat{H}_{El,-ph}^{MF} = -\sum_{ij\sigma} \left(\Delta_{ij\sigma} a_{i\sigma}^+ a_{j-\sigma}^+ + \Delta_{ij\sigma}^* a_{j-\sigma} a_{i\sigma} \right). \tag{4.8}$$

Now let us consider the Fourier transform for gap function (4.7), taking into account that $a_{i\sigma} = \frac{1}{\sqrt{N}} \sum_k e^{ikR_i} a_{k\sigma}$ and $V_{k_1}^{el.-ph}$ is the Fourier transform of the electron-phonon coupling parameter, where N is the number of SC sites. Then we have

$$\Delta_{ij\sigma} = V_{ij}^{el.-ph} < a_{j-\sigma} a_{i\sigma} > =$$
$$= \frac{1}{N^2} \sum_{k_1 q q_1} V_{k_1}^{el.-ph} e^{ik_1(R_i - R_j)} e^{iqR_j} e^{iq_1 R_i} < a_{q-\sigma} a_{q_1\sigma} > \delta_{q_1,-q} = \tag{4.9}$$
$$= \frac{1}{N} \sum_k e^{ik(R_i - R_j)} \sum_q V_{k-q}^{el.-ph} < a_{-q-\sigma} a_{q\sigma} >,$$

where the sum over k_1 is replaced by the sum over $k = k_1 + q$ and the Kronecker symbol determines the gap homogeneity. Thus, from (4.9) we obtain an expression for the Fourier transform of the gap function

$$\Delta_{k\sigma} = \sum_q V_{k-q}^{el.-ph} < a_{-q-\sigma} a_{q\,\sigma} > \tag{4.10}$$

The expression (4.10) defines a self-consistent equation for the gap function, since the abnormal means according to Eq. (4.8) are also expressed in terms of $\Delta_{ij\sigma}$. Standard methods for solving the problem of finding the gap are based on the diagonalization of Hamiltonian (4.8) in a wave space (BCS Hamiltonian) using the Bogolyubov transformation. Unfortunately, such diagonalization does not work for hybrid structures. As a rule, the Gor'kov equations for the coordinate Green's functions are considered, which in the general case are inhomogeneous. It causes considerable difficulties in calculating the nonlinear contributions. In [4.11], we described a method based on averaging over the unperturbed site Hamiltonians

$$\hat{H}_{0N} = -\sum_{i\sigma} \mu_\sigma c_{\sigma i}^+ c_{\sigma i} \,, \tag{4.11}$$

$$\hat{H}_{0S} = -\mu_2 \sum_{i\sigma} a_{\sigma i}^+ a_{\sigma i} \tag{4.12}$$

for N-metal and SC, respectively. In this case, the calculation of correlators in a site representation for series of the time perturbation theory with perturbations $V_N = \hat{H}_N - \hat{H}_{0N}$, $V_S = \hat{H}_S - \hat{H}_{0S}$ and $\hat{H}_T$ for FMM, SC and tunnel Hamiltonian $\hat{H}_T$, respectively, do not present any difficulties. Also, $\hat{H}_T$ is written in a site representation as

$$\hat{H}_T = \sum_{il\sigma} \left\{ T_{il} c_{i\sigma}^+ a_{l\sigma} + T_{il}^* a_{l\sigma}^+ c_{i\sigma} \right\}, \tag{4.13}$$

where T_{il} is an interstitial tunnel matrix element. Thus, it is possible to form infinite series of expansions for the Green's functions using the scattering matrix. After the Fourier transform of both the Matsubara unperturbed Green's functions and interaction parameters, the integration over time and site summation is easily performed. This ultimately gives an infinite series of algebraic expressions for the complete Green's functions easily summed for a certain type of diagrams. In particular, in the zeroth approximation over the inverse effective interaction radius, when loop diagrams are not taken into account, it is easy to summarize diagrams of the same type graphically within the framework of the well-known Dyson equation.

4.3 Equations for Green's functions and order parameters of a superconductor

In accordance with Hamiltonians (4.11)–(4.12), Fourier transforms of the unperturbed Matsubara causal Green's functions for N-metal and a superconductor have the form:

$$\tilde{G}_{1\sigma}(i\omega_n) = - < T_\tau c_{p\sigma}(\tau)c_{p\sigma}^+(0) >_{0,i\omega_n} = \frac{1}{\beta(i\omega_n + \mu_\sigma)} = -\tilde{G}_{2\sigma}(-i\omega_n)$$

$$G_{1\sigma}(i\omega_n) = - < T_\tau a_{q\sigma}(\tau)a_{q\sigma}^+(0) >_{0,i\omega_n} = \frac{1}{\beta(i\omega_n + \mu_2)} = -G_{2\sigma}(-i\omega_n) \quad , \tag{4.14}$$

where the symbol $<....>_0$ denotes an averaging with Hamiltonians (4.11) or (4.12). The imaginary frequency $i\omega_n=i\pi(2n+1)/\beta$ and $1/\beta=T$ is the temperature.

To find the abnormal correlator $<a_{-q-\sigma}a_{q\sigma}>$, which determines the spontaneous order parameter in an SC, it is necessary to enter the total causal Green's functions:

$$Z_{-q-\sigma}^{--}(\tau) = - < Ta_{-q-\sigma}(\tau)a_{q\sigma}(0) >, \; Z_{q\sigma}^{+-}(\tau) = - < Ta_{q\sigma}^+(\tau)a_{q\sigma}(0) >,$$

$$Y_{-pq-\sigma}^{--}(\tau) = - < Tc_{-p-\sigma}(\tau)a_{q\sigma}(0) >, \; Y_{pq\sigma}^{+-}(\tau) = - < Tc_{p\sigma}^+(\tau)a_{q\sigma}(0) >, \tag{4.15}$$

In the zero approximation for a self-consistent field, the above Green's functions are interconnected by means of graphical equations in the Fourier space as shown in Fig. 4.1 where the wave lines correspond to interactions according to (4.1), and thin and bold straight lines reflect the frequency dependent Green's functions (4.14) and (4.15) [4.11], respectively. Bold dots represent sums over the inner momenta of the diagram. In the analytical form, these equations are written as follows:

$$Z_{-q-\sigma}^{--}(i\omega_n) = \beta G_1(i\omega_n)\left(\varepsilon_{2-q}Z_{-q-\sigma}^{--}(i\omega_n) + \Delta_{q\sigma}Z_{q\sigma}^{+-}(i\omega_n) + \sum_p T_{-p-q}^* Y_{-pq-\sigma}^{--}(i\omega_n) \right)$$

$$Z_{q\sigma}^{+-}(i\omega_n) = G_2(i\omega_n) - \beta G_2(i\omega_n)\left(\varepsilon_{2q}Z_{q\sigma}^{+-}(i\omega_n) - \Delta_{q\sigma}^* Z_{-q-\sigma}^{--}(i\omega_n) + \sum_p T_{pq}Y_{pq\sigma}^{+-}(i\omega_n) \right)$$

$$Y_{-pq-\sigma}^{--}(i\omega_n) = \beta \tilde{G}_{1-\sigma}(i\omega_n)\left(\varepsilon_{1-p}Y_{-pq-\sigma}^{--}(i\omega_n) + T_{-p-q}Z_{-q-\sigma}^{--}(i\omega_n) \right)$$

$$Y_{pq\sigma}^{+-}(i\omega_n) = \beta \tilde{G}_{2\sigma}(i\omega_n)\left(-\varepsilon_{1p}Y_{pq\sigma}^{+-}(i\omega_n) - T_{pq}^* Z_{q\sigma}^{+-}(i\omega_n) \right), \tag{4.16}$$

where $\varepsilon_{1p} = \varepsilon_{1-p}$, $\varepsilon_{2q} = \varepsilon_{2-q}$ and T_{pq} are Fourier transforms of the hopping integrals t_{1ij} and t_{2ij} for N-metal, SC and tunnel matrix element, respectively. Note that the momentum **p** always refers to a N-metal, and **q** to SC.
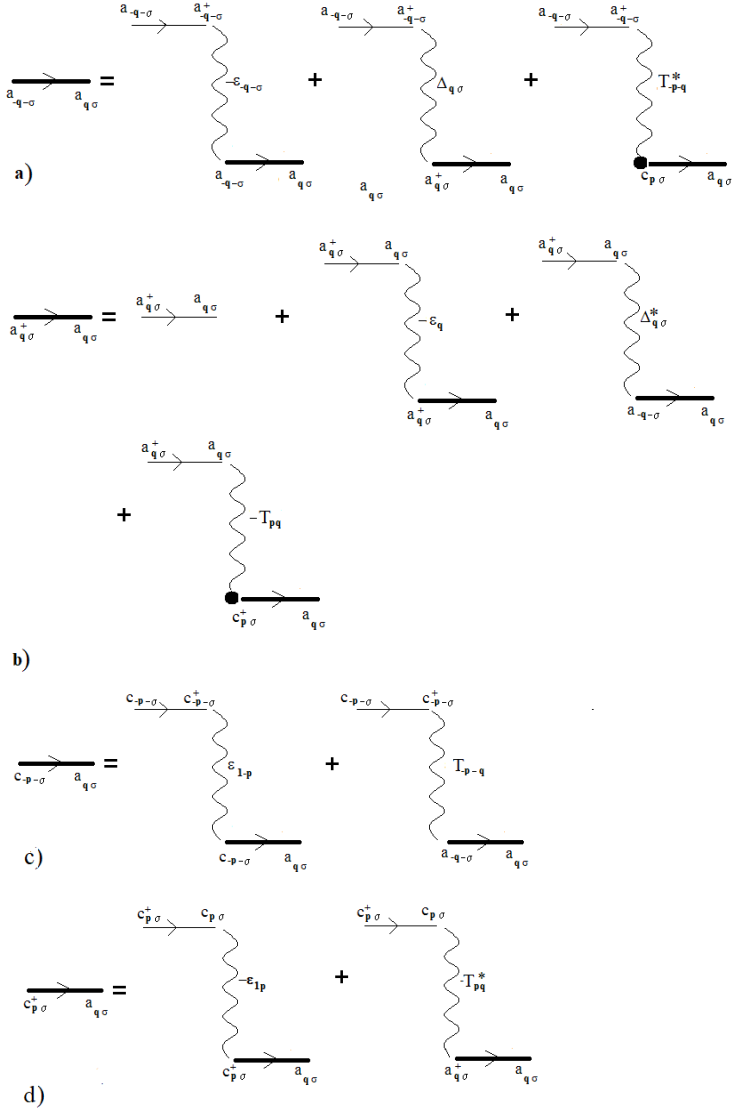
Fig. 4.1 – Graphic system of equations for total causal Green's functions $Z_{-q-\sigma}^{--}(i\omega_n)$, $Z_{q\sigma}^{+-}(i\omega_n)$, $Y_{-pq-\sigma}^{--}(i\omega_n)$ and $Y_{pq\sigma}^{+-}(i\omega_n)$, which determine the spontaneous order parameter $<a_{-q-\sigma}a_{q\sigma}>$ of the superconductor

137

From the system of Eqs. (4.16), in the absence of tunneling, when $T_{il} = 0$, the trivial solutions $Y^{--}_{-pq\text{-}\sigma}(i\omega_n) = 0$ and $Y^{+-}_{pq\sigma}(i\omega_n) = 0$, and the first two equations coincide with the Gor'kov equations. Taking tunneling into account, the system becomes integral and describes nonlinear proximity effects, since it includes infinite series of contributions to the Green's functions from the tunneling matrix element. Despite the integral character of the system in Eqs. (4.16), it can be easily solved. To do this, from the 3-rd and 4-th equations we find the unknown $Y^{--}_{-pq\text{-}\sigma}(i\omega_n)$ and $Y^{+-}_{pq\sigma}(i\omega_n)$ and substitute them into the first two equations of the above system, that gives us

$$Z^{--}_{-q\text{-}\sigma}(i\omega_n) = \frac{\Delta_{q\sigma} / \beta}{\left[i\omega_n - \xi_q - \tilde{\varphi}_{1-\sigma}(i\omega_n)\right]\left[i\omega_n + \xi_q - \tilde{\varphi}_{2\sigma}(i\omega_n)\right] - \left|\Delta_{q\sigma}\right|^2},$$

$$Z^{+-}_{q\sigma}(i\omega_n) = \frac{\left[i\omega_n - \xi_q - \tilde{\varphi}_{1-\sigma}(i\omega_n)\right] / \beta}{\left[i\omega_n - \xi_q - \tilde{\varphi}_{1-\sigma}(i\omega_n)\right]\left[i\omega_n + \xi_q - \tilde{\varphi}_{2\sigma}(i\omega_n)\right] - \left|\Delta_{q\sigma}\right|^2}$$

(4.17)

where $\xi_q = \varepsilon_{2q} - \mu_2$ is the band energy of electrons relatively the Fermi level of the SC.

It is easy to see from expressions (4.17) for the Green's functions that the excitation spectrum of a superconductor in a hybrid structure is incoherent, since $\tilde{\varphi}_{1-\sigma}(\omega)$ and $\tilde{\varphi}_{2\sigma}(\omega)$ contain the finite imaginary parts (see below), determined by the tunnel matrix element.

The functions $\tilde{\varphi}_{1-\sigma}(i\omega_n)$ and $\tilde{\varphi}_{2\sigma}(i\omega_n)$, which determine an FMM effect on a superconductor, are as follows:

$$\tilde{\varphi}_{1-\sigma}(i\omega_n) = \sum_p \frac{\left|T_{pq}\right|^2}{i\omega_n + (\mu_2 - \varepsilon_{1p})}$$

$$\tilde{\varphi}_{2\sigma}(i\omega_n) = \sum_p \frac{\left|T_{pq}\right|^2}{i\omega_n - (\mu_\sigma - \varepsilon_{1p})}$$

(4.18)

Using the Green's functions (4.17), one can find spontaneous SC gap function by Eq. (4.11)

$$< a_{-q\text{-}\sigma} a_{q\sigma} > = -\beta \sum_i \text{Res}\left[Z^{--}_{-q\text{-}\sigma}(\omega)(f(\omega)-1)\right]\Big|_i.$$

(4.19)

Here the symbol Res[…] denotes the residues of the Green's function $Z_{-q-\sigma}^{--}(\omega)$ with a factor $f(\omega)-1$, $f(\omega)=1/(\exp(\omega/T)+1)$ is the Fermi distribution function. The analytical continuation $i\omega_n \rightarrow \omega+i\delta$ for $Z_{q\sigma}^{+-}(i\omega_n)=-Z_{q\sigma}^{-+}(-i\omega_n)$ allows us to find a spectrum and a spectral density of electron-hole excitations of the Cooper pair's condensate:

$$R_\sigma(\boldsymbol{q},\omega)=-2\beta \operatorname{Im} Z_{q\sigma}^{-+}(\omega+i\delta) , \tag{4.20}$$

the coherence degree is controlled by the imaginary part of its poles. Obviously, the scattering of electrons depends only on the tunnel barrier.

Note that the remaining Green's functions describe hoppings of the condensate electrons and holes from SC to N-metal. Indeed, from Eq. (4.16) it follows

$$Y_{-pq-\sigma}^{--}(i\omega_n) = \frac{\beta T_{-p-q}\tilde{G}_{1-\sigma}(i\omega_n)}{1-\beta\varepsilon_{1p}\tilde{G}_{1-\sigma}(i\omega_n)} Z_{-q-\sigma}^{--}(i\omega_n)$$
$$Y_{pq\sigma}^{+-}(i\omega_n) = -\frac{\beta T_{pq}^*\tilde{G}_{2\sigma}(i\omega_n)}{1+\beta\varepsilon_{1p}\tilde{G}_{2\sigma}(i\omega_n)} Z_{q\sigma}^{+-}(i\omega_n) \tag{4.21}$$

It can be seen from (4.21) that the indicated Green's functions are proportional to the tunnel matrix elements. The coherent spectrum of electron and hole excitations in an N-metal is expressed as $\omega_{p\sigma}=\pm(\varepsilon_{1p}-\mu_{-\sigma})$ with a quasiparticle peak to be determined by electron tunneling. These excitations correspond to the well-known Andreev reflection process, since they are realized for an arbitrary direction of the electron momentum. It turns out to be the excitations of Andreev reflections in SC are also coherent, since the corresponding Fourier component of the Green's function $Z_{qp\sigma}^{+-}(\tau)=-<Ta_{q\sigma}^+(\tau)c_{p\sigma}(0)>$ has poles determined by zeros of the function [4.11]:

$$d_{q\sigma}(\omega) = \frac{(\omega-E_{q\sigma})(\omega+E_{q\sigma})}{\omega^2-\mu_2^2} , \tag{4.22}$$

where $E_{q\sigma}=\sqrt{(\varepsilon_q-\mu_2)^2+|\Delta_{q\sigma}|^2}$ is the spectrum of electron excitations with Cooper pairing, which do not depend on the tunnel matrix element.

To determine the spontaneous gap accordingly to Eq. (4.19), after the analytic continuation $\omega \rightarrow \omega + i\delta$, it is necessary to calculate the functions $\tilde{\varphi}_{1-\sigma}(\omega)$ and $\tilde{\varphi}_{2\sigma}(\omega)$. Obviously, these functions are connected by the relation

$$\tilde{\varphi}_{1-\sigma}(\omega) = -\tilde{\varphi}_{2-\sigma}(-\omega) \tag{4.23}$$

Next, we consider the simplest case $|T_{pq}|^2 = |B|^2$, when the tunnel matrix element does not depend on the wave vectors. The frequency ω is supposed to be complex valued and $|\omega/\mu_1| \ll 1$. Taking into account that the electron density of states $\rho_S(\varepsilon) = C_S\sqrt{\varepsilon}$ with the constant C_S proportional to the volume V_N of the N-metal, the calculation of integrals (4.18) is elementary and we obtain:

$$\begin{aligned}
\tilde{\varphi}_{1-\sigma}(\omega) &= \varphi_0(\omega, \Gamma_N) = -\Gamma_N \left(2 + \ln\left(\frac{\omega}{4\mu_1} \right) \right) \\
\tilde{\varphi}_{2\sigma}(\omega) &= \Gamma_N \left(2 + \ln\left(\frac{-\omega}{4\mu_1} \right) \right)
\end{aligned} \tag{4.24}$$

where the value $\Gamma_N = |B|^2 \rho_N(\mu_1)$ determines the barrier transparency for FMM electrons. It is also clear that the contribution from magnetism under the sign of the logarithm is infinitesimal of a higher order than $|\omega/\mu_1|$. Therefore, an influence of the N-metal magnetic ordering on SC can be neglected and spin indices in Eq. (4.24) may be disregarded. Since the branch cut of complex functions (4.24) lies on the negative frequency axis ω, it is necessary to take into account the following relation:

$$\ln(\omega) - \ln(-\omega) = i\pi\, sign(\arg \omega) \tag{4.25}$$

One can write an equation for pole singularities of the Green's functions (4.17) and find the gap in SC:

$$\omega^2 - \omega\left[\tilde{\varphi}_1(\omega) + \tilde{\varphi}_2(\omega)\right] + \xi_q\left[\tilde{\varphi}_2(\omega) - \tilde{\varphi}_1(\omega)\right] + \tilde{\varphi}_1(\omega)\tilde{\varphi}_2(\omega) - \xi_q^2 - |\Delta_{q\sigma}|^2 = 0, \tag{4.26}$$

where $\tilde{\varphi}_{1-\sigma}(\omega) = \tilde{\varphi}_1(\omega)$ and $\tilde{\varphi}_{2\sigma}(\omega) = \tilde{\varphi}_2(\omega)$ in accordance with aforesaid. Formally, this equation can be considered as quadratic with respect to the complex frequency ω. It allows to write the implicit solution in the form

$$\omega_{q\sigma}^{\pm} = -\frac{1}{2}i\pi\Gamma_N sign(\arg \omega_{q\sigma}^{\pm}) \pm \sqrt{\left(\xi_q - \Gamma_N\left(2 + \ln\left[\frac{\omega_{q\sigma}^{\pm}}{4\mu_1}\right]\right) + \frac{1}{2}i\pi\Gamma_N sign(\arg \omega_{q\sigma}^{\pm})\right)^2 + \left|\Delta_{q\sigma}\right|^2} \quad (4.27)$$

Unfortunately, Eq. (4.27) is transcendental relative to the unknown $\omega_{q\sigma}^{\pm}$. However, it is easy to obtain solutions for both electron and hole excitations by the iteration procedure. As a start, it is necessary to set $\omega_{q\sigma} = E_{q\sigma} + i\delta$ that corresponds to the analytic continuation of the Green's functions to the complex upper half-plane. The iterative procedure for calculating the roots determines solutions with imaginary parts of the opposite sign for each root. This uncertainty for the roots appears due to the replacement $\omega \rightarrow \omega + i\delta$ at the analytic continuation of Green's functions (4.17) for each iteration step in Eq. (4.27) because logarithm gives roots on opposite edges of the branch cut. It is clear that the first step of the iteration determines the sign of the imaginary part of the pole, and the next step of the opposite sign is associated with the violation of the selected condition for interaction adiabatic switching on. It is interesting to note that in [4.12] only the 1-st iteration step was applied to Eq. (4.27). As will be shown below, the rigorous self-consistency over frequencies $\omega_{q\sigma}^{\pm}$ drastically changes the order parameters pointing out on a significant contribution $\ln\left[\omega_{q\sigma}^{\pm}/4\mu_1\right]$ to the proximity effect in the FMM-SC structure.
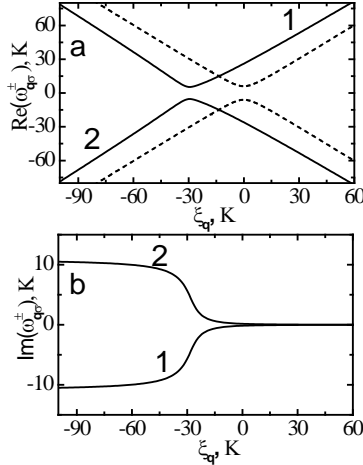
Fig. 4.2 – Real (a) and imaginary (b) parts of the electron and hole excitations spectrum $\omega_{q\sigma}^{+}$ and $\omega_{q\sigma}^{-}$ (solid curves 1 and 2, respectively) for the FMM-SC hybrid structure, $\Delta = 6$ K, $\Gamma_N = 3.495$ K and $\mu = 6$ eV, as well as the corresponding coherent BCS spectrum (dashed curves)

Fig. 4.2 shows real and imaginary parts of the poles as a function of the electron energy ξ_q relative to the Fermi energy level for the gap $\Delta = 6$ K, barrier transparency $\Gamma_N = 3.49$ K and $\mu_1 = 6$ eV (solid lines). The BCS spectrum (dashed line) is demonstrated for comparison.

To find the solution $\Delta_{q\sigma}$ from Eq. (4.10) after finding the self-consistent solutions $\omega_{q\sigma}^+ = \omega_{q\sigma}$ and $\omega_{q\sigma}^- = -\omega_{q\sigma}$ for the poles $Z_{-q-\sigma}^-(\omega)$ from Eq. (4.19), it is necessary to make an obvious replacement $\tilde{\varphi}_1(\omega) = \tilde{\varphi}_1(\omega_{q\sigma}^+)$ and $\tilde{\varphi}_2(\omega) = \tilde{\varphi}_2(\omega_{q\sigma}^+)$ in Eq. (4.26). Note that Eq. (4.26) is invariant under the substitution $\omega_{q\sigma}^+ \to \omega_{q\sigma}^-$ (see Eq. (4.23)). Thus, the anomalous Green's function takes the simplest form

$$Z_{-q-\sigma}^{--}(i\omega_n) = \frac{\Delta_{q\sigma}/\beta}{\left(i\omega_n - \omega_{q\sigma}\right)\left(i\omega_n + \omega_{q\sigma}\right)}, \tag{4.28}$$

that gives the order parameter

$$<a_{-q-\sigma}a_{q\sigma}> = \frac{\Delta_{q\sigma}}{2\omega_{q\sigma}}\tanh\left(\frac{\omega_{q\sigma}}{2T}\right). \tag{4.29}$$

The gap function is a complex value for $\Gamma_N \neq 0$, and for $\Gamma_N = 0$ it coincides with the BCS theory result. Then, according to Eq. (4.10), we obtain a self-consistent equation for the complex gap $\Delta_{q\sigma}$:

$$\Delta_{k\sigma} = \sum_q V_{k-q}^{el.-ph} \frac{\Delta_{q\sigma}}{2\omega_{q\sigma}}\tanh\left(\frac{\omega_{q\sigma}}{2T}\right) \tag{4.30}$$

Assuming that the electron-phonon interaction parameter $V_{k-q}^{el.-ph} = U$ is nonzero near the Fermi level in a narrow energy region of the order of $\pm \omega_D$, where ω_D is the Debye frequency, let us denote the electron-phonon coupling constant for SC by $\lambda = \rho_F(\mu_2)U$. Here $\rho_F(\mu_2)$ is the electron density of states at the Fermi surface. Obviously, $\rho_F(\mu_2)$ does not depend on the sample volume. Then one can obtain the integral complex equation for the spontaneous gap

$$\Delta_{k\sigma} = \lambda \int_{-\omega_D}^{\omega_D} \frac{\Delta_{q\sigma}}{2\omega_{q\sigma}}\tanh\left(\frac{\omega_{q\sigma}}{2T}\right)d\xi_q \tag{4.31}$$

In the simple case of the s-wave gap with a spatially homogeneous phase, $\Delta_{k\sigma} = \Delta = \Delta_S e^{i\varphi}$, where $\Delta_S = |\Delta_{k\sigma}|$, and φ is determined by the rest of the integrand

in Eq. (4.31), which depends on Γ_N. In the approximation $\varphi = $ const and at $\Gamma_N = 0$, this phase is equal to zero. For a gap under the integral one can put $\Delta_{q\sigma} = \Delta_s e^{i0}$. Taking the modulus from both sides of Eq. (4.31) with account for the indicated replacement, we obtain the equation for the gap modulus:

$$1 = \lambda \left| \int_{-\omega_D}^{\omega_D} \frac{1}{2\omega_{q\sigma}} \tanh\left(\frac{\omega_{q\sigma}}{2T}\right) d\xi_q \right|, \tag{4.32}$$

Since the modulus of the right-hand side of Eq. (4.32) is equal to 1, it can be assumed that the corresponding complex number also determines the gap phase φ that makes it possible to write

$$\varphi = \arg\left(\lambda \int_{-\omega_D}^{\omega_D} \frac{1}{2\omega_{q\sigma}} \tanh\left(\frac{\omega_{q\sigma}}{2T}\right) d\xi_q \right) \tag{4.33}$$

Thus, using Eqs. (4.32)–(4.33), it is able to calculate an absolute value of the spontaneous gap Δ_S of SC, its phase φ, and the critical temperature T_C of the phase transition, taking into account an influence of the effects of incoherent electrons tunneling in a normal metal.

In Fig. 4.3a, the dependence of the spontaneous gap Δ_S of the Sn superconductor on the barrier transparency Γ_N at the temperature $T = 0$ (solid curve), which describes an inverse proximity effect, is shown. The dashed curve was obtained for the poles in Eq. (4.27) obtained at the first step of the iteration [4.12].

The critical value of transparency $\Gamma_N = \Gamma_N^{cr} = 3.495$ K, above which superconductivity is destroyed, is determined from the equation for T_C at $\tanh\left(\frac{\omega_1(\xi_q)}{2T}\right) = 1$:

$$F(T,\Gamma_N) = \lambda \left| \int_{-\omega_D}^{\omega_D} \frac{1}{2\omega_1(\xi_q)} \tanh\left(\frac{\omega_1(\xi_q)}{2T}\right) d\xi_q \right| - 1 = 0, \tag{4.34}$$

where the frequency $\mathrm{Re}(\omega_1(\xi_q)) > 0$ and $\omega_1(\xi_q)$ is the self-consistent solution of Eq. (4.27) at $|\Delta_{q\sigma}| = 0$. Near the high transparency a role of cooperative phenomena associated with electron-hole scattering by a barrier increases significantly, that is indicated by the order parameter phase (see Fig. 4.3b). On

the other hand, the temperature fluctuations partially stabilize the superconducting state, since high-energy electrons from the normal metal are more strongly dissipated. Therefore, with decreasing temperature, an area of the ordered phase for a highly transparent barrier narrows. In general, the state of itinerant electrons itself is rather complex, that is reflected in the form of a nonmonotonic behavior of the phase transition critical temperature T_C, as well as an appearance of the reentrant superconductivity in certain temperature areas.
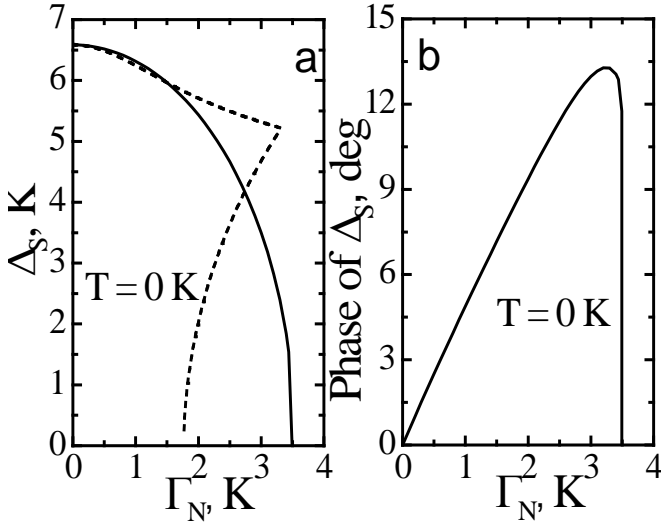
Fig. 4.3 – Dependence of the spontaneous gap Δ_S (a) and its phase (b) of superconductor Sn on the barrier transparency Γ_N at the temperature $T = 0$ (solid curve).
The dashed curve reflects the same dependence but without self-consistency over the poles from Eq. (4.27) (the first iteration step in Eq. (4.27) [4.12]).
The parameters values for tin are as follows: $\lambda = 0.245$, $\omega_D = 195$ K, $\mu_1 = 6$ eV

Fig. 4.4 shows that the critical temperature T_C at $\Gamma_N \sim \Gamma_N^{cr}$ for FMM-Sn and FMM-Pb hybrid structures is the multiple-valued function of Γ_N. Also, T_C strongly fluctuates relative to small changes in Γ_N, when approaches the zero temperature. With further growth Γ_N, T_C even increases but in this case, superconductivity at low temperatures disappears, and the high-temperature area of the nonzero order parameter gradually narrows to zero.
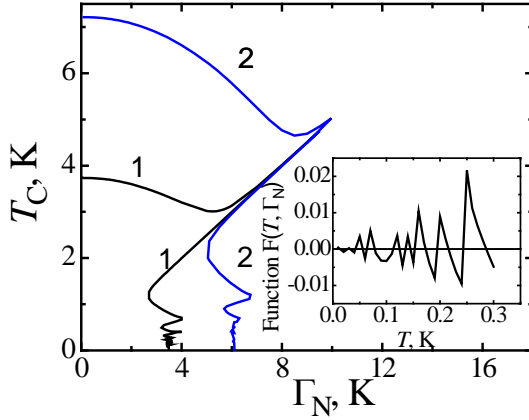
Fig. 4.4 – Phase diagram of FMM-Sn and FMM-Pb structures (curves 1 and 2, respectively). For Pb, the values $\mu_2 = 9.9$ eV, $\lambda = 0.39$, $\Gamma_N^{cr} = 6.105$ K and $\omega_D = 96$ K are taken. The inset shows the function $F(T, \Gamma_N)$ from Eq. (4.34) at $\Gamma_N = \Gamma_N^{cr} = 3.495$ and low T, the zeros of which determine T_C of the superconductor
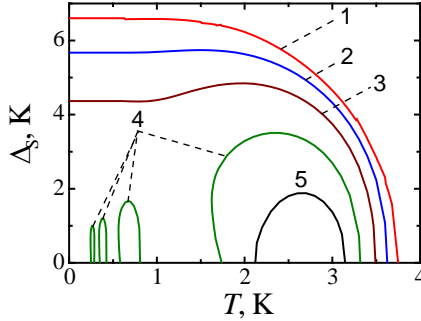
Fig. 4.5 – Temperature dependences of the spontaneous gap Δ_S of the normal metal-tin structure at barrier transparency values $\Gamma_N = 0$, 1.8, 2.65, 3.495, and 4.25 K (curves 1–5, respectively) with the parameter values from Fig. 4.3

In Fig. 4.5, temperature dependences of the gap Δ_S of tin in N-metal-Sn hybrid structure are shown for different values of the barrier transparency Γ_N. It can be seen from the figure that at $\Gamma_N \sim \Gamma_N^{cr}$ the order parameter exists in certain temperature regions, *i. e.*, in this case an emergence of reentrant super-conductivity is possible. With decreasing temperature, as well as with in-creasing Γ_N, the area of the superconductivity existence narrows. Also, near one of the critical temperatures, a two-gap state is possible, that may indicate a first-order phase transition. Since the phase of the gap is directly related to

the incoherent scattering of tunnel electrons by the barrier, its temperature dependences for different transparencies Γ_N are of interest.

Figure 4.6 shows temperature dependences of phases for gap functions from Fig. 4.5. It can be seen that the phase near the "left" critical temperature, increases sharply while near the "right" one, it decreases monotonically until abruptly disappearing when $\Delta_S = 0$. Thus, the presented dependences T_C and Δ_S reflect complex nature of the relationship between incoherent tunneling electron scattering, thermal fluctuations, and coherent Cooper pairing.
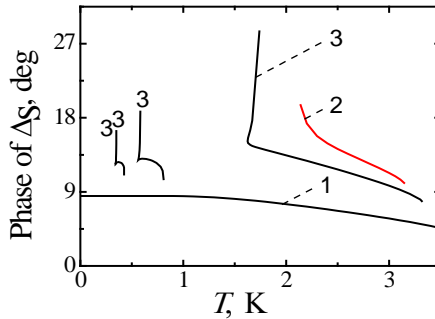
Fig. 4.6 – Temperature dependences of the gap phase φ with moduli Δ_S from Fig. 4.5 for transparencies Γ_N = 1.8, 3.495 and 4.25 K (curves 1–3, respectively) and with the parameter values from Fig. 4.3
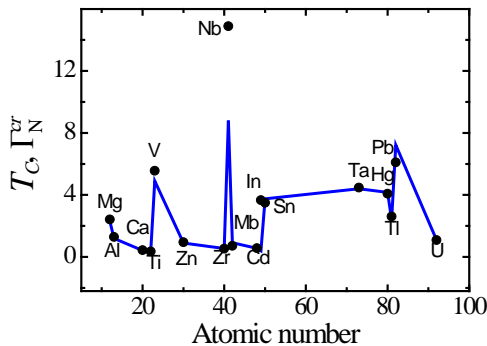
Fig. 4.7 – Critical barrier transparencies Γ_N^{cr} (points) and temperatures T_C (top of the broken line) [4.15] for various metals

In Fig. 4.7, critical temperatures (according to the data of Ref. [4.15]) and the calculated transparencies Γ_N^{cr} for series of superconductors are shown. It can be seen that with the exception of Nb, the values of T_C and Γ_N^{cr} differ

insignificantly. Thus, one can say that the critical barrier transparency is mainly determined by the value of T_C, and the reentrant superconductivity is possible with such a high transparency.

The expression for the spectral density of states $R_\sigma(\boldsymbol{q},\omega)$ from Eq. (4.20) takes the form:

$$R_\sigma(\boldsymbol{q},\omega) = -2\pi\Gamma_N \frac{\theta(\omega)\left[\omega^2 - \tilde{E}_q^2\right] - (\omega + \tilde{\xi}_q)(\omega - sign(\omega)\tilde{\xi}_q)}{\left[\omega^2 - \tilde{E}_q^2\right]^2 + \pi^2\Gamma_N^2(\omega - sign(\omega)\tilde{\xi}_q)^2}, \tag{4.35}$$

where $\tilde{E}_{q(\omega)} = \sqrt{\tilde{\xi}_q^2(\omega) + \Delta_s^2}$, $\tilde{\xi}_q(\omega) = \xi_q + \varphi_0(|\omega|, \Gamma_N)$, $\theta(\omega)$ is the Heaviside step function, and $\varphi_0(\omega, \Gamma_N)$ is the function from Eqs. (4.24). Let us define the homogeneous spectral density as

$$R_U^s(\omega) = \sum_{\boldsymbol{q}} R_\sigma(\boldsymbol{q},\omega) = \rho_S(\mu_2) \int_{-\omega_D}^{\omega_D} d\xi_q R_\sigma(\boldsymbol{q},\omega), \tag{4.36}$$

where $\rho_S(\mu_2)$ is the bulk electron density of states of a SC metal at the Fermi level.
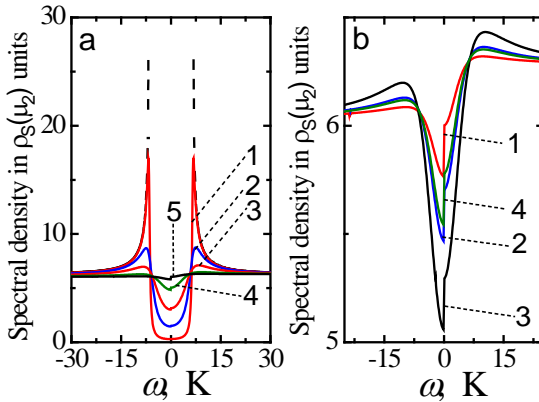
Fig. 4.8 – Frequency dependences of the homogeneous spectral density $\tilde{R}(\omega)$ from Eq. (4.35) in units $\rho_S(\mu_2)$ for the superconductor in a hybrid structure "normal metal-Sn": a) at the temperature $T = 0$ and $\Gamma_{N=0}$ ($\Delta_S = 6.6$ K, dashed line), 0.2, 1.0, 2.0, 3.0 and 3.44 K ($\Delta_S = 6.57, 6.32, 5.44, 3.50, 1.54$, solid lines 1–5, respectively); b) at the critical transparency $\Gamma_N = \Gamma_N^{cr} = 3.495$ K and $T = 1.625, 1.7, 2.4, 3.1$ ($\Delta_S = 1.7, 2.53, 3.51, 2.34$, curves 1–4, respectively)

In Fig. 4.8 the frequency dependences of a homogeneous spectral density of the superconductor Sn at the temperature $T = 0$ K for different Γ_N values and at critical transparency $\Gamma_N = \Gamma_N^{cr} = 3.495$ K in the temperature area from 1.6 to 3.1 K, where the reentrant superconductivity is realized, are shown. It can be seen from Fig. 4.8a that for small Γ_N the $R_U^S(\omega)$ is close to the conventional $R_\sigma^S(\omega)$ for a homogeneous superconductor:

$$R_\sigma^S(\omega) = \frac{2\pi\rho_s(\mu_2)|\omega|}{\sqrt{\omega^2 - \Delta_S^2}} \tag{4.37}$$

With increasing Γ_N, the spectral density $\tilde{R}(\omega)$ approaches the value of $2\pi\rho_s(\mu_2)$ that corresponds to N-metal and reflects the inverse proximity effect. In Fig. 4.7b, $\tilde{R}(\omega)$ is shown at the critical transparency $\Gamma_N^{cr} = 3.495$ K, and in the temperature area of the reentrant superconductivity appearance. It can be seen from the figure that in this case, due to a high barrier transparency, an influence of the N-metal on the spontaneous order parameter is quite significant. Also, due to the jump at the singular point $\omega = 0$, $\tilde{R}(\omega)$ is asymmetric near the origin. The presented dependences are in a good agreement with the known experimental data [4.16].

4.4 Proximity effect in a ferromagnetic metal

In this subsection, we will consider an influence of SC on a FMM, *i. e.*, a proximity effect associated with the emergence of an induced gap in the specified metal. It was shown above, that the magnetic order of an N-metal has a negligible effect on the SC. It turns out that the SC significantly affects both transport in a metal due to the proximity effect and its spectral properties. In a similar way, we can obtain expressions for corresponding electron Green's functions of a metal using the induced order parameter $<c_{-p-\sigma}c_{p\sigma}>$, spectrum of excitations, and their damping. The details are presented in the work [4.11]. Therefore, we can write down the expressions for the Fourier transforms of the retarded anomalous $Y_{p\sigma}^{--}(\tau) = -<Tc_{-p-\sigma}(\tau)c_{p\sigma}(0)>$ and conventional $Y_{p\sigma}^{-+}(\tau) = -<Tc_{p\sigma}(\tau)c_{p\sigma}^{+}(0)>$ Green's functions of the N-metal:

$$Y_{p\sigma}^{--}(\omega+i\delta) = -\frac{1}{\beta}\frac{\tilde{\beta}\ (\omega+i\delta)}{\Omega_{p\sigma}(\omega+i\delta)}$$

$$Y_{p\sigma}^{-+}(\omega+i\delta) = \frac{1}{\beta}\frac{\omega+i\delta+\xi_p+J_0\sigma-\tilde{\gamma}\ (\omega+i\delta)}{\Omega_{p\sigma}(\omega+i\delta)} \quad (4.38)$$

where

$$\Omega_{p\sigma}(\omega+i\delta) = (\omega+i\delta+\xi_p-J_0\sigma-\tilde{\gamma}\ (\omega+i\delta))(\omega+i\delta-\xi_p-J_0\sigma-\tilde{\alpha}\ (\omega+i\delta))-\left|\tilde{\beta}\ (\omega+i\delta)\right|^2, \quad (4.39)$$

$\xi_p = \varepsilon_{1p}-\mu_1$, $\Gamma_S = \rho_S(\mu_2)B^2$ is the barrier transparency for SC condensate electrons. Also, we have the following equations

$$\tilde{\alpha}(\omega) = -\Gamma_S\left\{2+\ln\frac{b(\omega)}{4\mu_2}+\frac{1}{2}i\pi\left[\frac{\omega}{b(\omega)}sign(\arg(b(\omega)))+sign(\arg(-b(\omega)))\right]\right\}$$

$$\tilde{\beta}(\omega) = -\Delta\Gamma_S\frac{i\pi}{2b(\omega)}sign(\arg(b(\omega))) \quad\quad , \quad (4.40)$$

$$\tilde{\gamma}(\omega) = \Gamma_S\left\{2+\ln\frac{b(\omega)}{4\mu_2}-\frac{1}{2}i\pi\left[\frac{\omega}{b(\omega)}sign(\arg(b(\omega)))-sign(\arg(-b(\omega)))\right]\right\}$$

where $b(\omega)=\sqrt{\omega^2-|\Delta|^2}$. The spectrum of excitations is found from pole singularities of the indicated Green's functions, *i. e.*, at the condition $\Omega_{p\sigma}(\omega+i\delta)=0$ that gives an equation for the resonance frequencies ω with account for the analytical continuation $\omega > \omega + i\delta$:

$$\omega-J_0\sigma = -\frac{1}{2}i\pi\Gamma_S\frac{\omega}{b(\omega)}sign\left(\arg\left[b(\omega)\right]\right)\pm$$

$$\pm\sqrt{\left(\xi_p-\Gamma_S\left(2+\ln\left[\frac{b(\omega)}{4\mu_2}\right]\right)-i\pi\Gamma_S sign\left(\arg\left[-b(\omega)\right]\right)\right)^2-\pi^2\Gamma_S^2\frac{|\Delta|^2}{4b^2(\omega)}} \quad (4.41)$$

The transcendental Eq. (4.41) has complex roots $\omega_{1\sigma p}$ and $\omega_{2\sigma p}$, which are determined numerically by the iteration procedure.
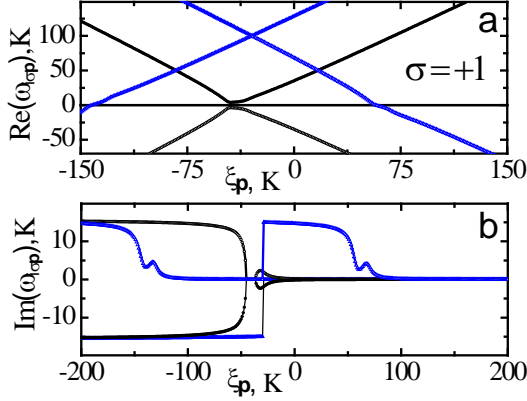
Fig. 4.9 – Real (a) and imaginary (b) parts of the excitation electron frequencies $\omega_{1\sigma p}$ (dark circles and triangles) and $\omega_{2\sigma p}$ (open circles and triangles) as functions of the electron energy ξ_p with the barrier transparency $\Gamma_S = 5$ K, the gap $\Delta_S = 6.6$ K and the ferromagnetic exchange $J_0 = 0$ and 100 K (circles and triangles, respectively)

Fig. 4.9 shows results of the calculations for $\omega_{1\sigma p}$ and $\omega_{2\sigma p}$ as a function of energy ξ_p for both paramagnetic and ferromagnetic N-metals. It can be seen that for a paramagnet in a certain range of values ξ_p and at frequencies $|\omega| < |\Delta|$, the gap is induced in the N-metal as a realization of the proximity effect with a nonzero anomalous order parameter $< c_{-p-\sigma} c_{p\sigma} >$, which is suppressed by the ferromagnetic exchange. Note that the correlator $< c_{-p-\sigma} c_{p\sigma} >$ does not depend on the electron-phonon coupling constant in the N-metal and is proportional to the gap Δ, since the N-metal is not a superconductor. On the whole, the spectrum is incoherent for nonzero Γ_S. At the same time, electron excitations with frequencies $|\omega| < |\Delta|$ are coherent. Let us consider this issue in more detail, since it is necessary for the correct calculation of the corresponding spectral density.

Indeed, it is easy to see that at $|\omega| < |\Delta|$ the tunnel functions (4.40) are real. The equation $\Omega_{p\sigma}(\omega) = 0$ is quadratic relatively unknown ξ_p for the integrand pole singularities of the homogeneous spectral density $R_U^N(\omega)$:

$$R_U^N(\omega) = \sum_p \tilde{R}_\sigma(\boldsymbol{p}, \omega) = \rho_N(\mu_1) \int_{-\tilde{\omega}_D}^{\tilde{\omega}_D} d\xi_p \tilde{R}_\sigma(\boldsymbol{p}, \omega), \qquad (4.42)$$

150

where $\tilde{R}_\sigma(\boldsymbol{p},\omega)=-2\beta\,\mathrm{Im}\,Y_{p\sigma}^{-+}(\omega+i\delta)$ and $\tilde{\omega}_D$ is Debye frequency for N-metal. That is why one can write its solutions $\xi_{1(\omega)}$ and $\xi_{2(\omega)}$ in the form:

$$\xi_{1,2}(\omega)=\Gamma_S\left(2+\ln\frac{\tilde{b}(\omega)}{4\mu_2}\right)\pm\sqrt{\left(\omega+J_0\sigma\right)\left(\omega+J_0\sigma+\Gamma_S\frac{\pi\omega}{\tilde{b}(\omega)}\right)-\frac{1}{4}\pi^2\Gamma_S^2}\;,\qquad(4.43)$$

where $\tilde{b}(\omega)=\sqrt{\Delta_S^2-\omega^2}$. Evidently, Eq. (4.43) gives poles on the real frequency axis if the radical expression is non-negative. Consider the simplest case $J_0=0$. Then at

$$\Gamma_S\leq\frac{2|\omega|\left\{|\omega|+\Delta_S\right\}}{\pi\sqrt{\Delta_S^2-\omega^2}}=g(\omega)\qquad(4.44)$$

we have the coherent spectrum, if $|\omega|<\Delta_S$ and $|\omega|>g^{-1}(\Gamma_S)=\omega_0(\Gamma_S)$, where $g^{-1}(x)$ is the inverse function from Eq. (4.44). The numerical analysis with analytical continuation $\omega\to\omega+i\delta$ shows that $sign(\mathrm{Im}(\xi_1(\omega+i\delta)))=sign(\omega)$ and $sign(\mathrm{Im}(\xi_2(\omega+i\delta)))=-sign(\omega)$. In accordance with the Landau bypass rule, it is easy to find the spectral density of coherent electron excitations in N-metal for frequencies $|\omega|<\Delta_S$.

$$R_U^N(\omega)=\frac{2\pi\,sign(\omega)\theta(|\omega|-\omega_0(\Gamma_S))\theta(\Delta_S-|\omega|)\rho_N(\mu_1)}{\sqrt{\omega\left(\omega+\Gamma_S\dfrac{\pi\omega}{\tilde{b}(\omega)}\right)-\dfrac{1}{4}\pi^2\Gamma_S^2}}\left\{\omega+\Gamma_S\frac{\pi\omega}{\tilde{b}(\omega)}\right\}.\qquad(4.45)$$

Fig. 4.10 shows the spectrum of coherent electronic excitations $\omega_{1,res}$ and $\omega_{2,res}$ from Eq. (4.43) in a paramagnetic N-metal at $\Delta_S=6.6$ K, $\Gamma_S=0.5$ and 5 K in the frequency region $|\omega_{i,res}|<\Delta_S$, as well as the corresponding homogeneous spectral densities of coherent and incoherent excitations from Eq. (4.41) at $|\omega_{i\sigma p}|>\Delta_S$. In Fig. 4.10a one can see that at $|\omega|<\Delta_S$ in the N-metal, a forbidden band is also formed. Its width depends both on the barrier transparency and on the SC gap. Also, in this case, the induced gap does not depend on the electron-phonon coupling constant in the N-metal. The main energy interval of electrons scattered by the barrier is assumed to be near the Fermi level with a width of the order of twice the Debye frequency. The spectral density in Fig. 4.10b reflects the coherence of the indicated excitations

with an increase in the quasiparticle peak as one approaches the boundaries of the forbidden band of the SC and N-metal. It is interesting to note that in the forbidden zone of the N-metal, *i. e.*, at $|\omega| < \omega_0(\Gamma_s)$, in contrast to the SC, there are purely complex poles of the Green's function $Y_{p\sigma}^{-+}(\omega + i\delta)$ that point out on strong electrons scattering. It can be shown that the corresponding spectral density is identically equal zero, as in the SC.
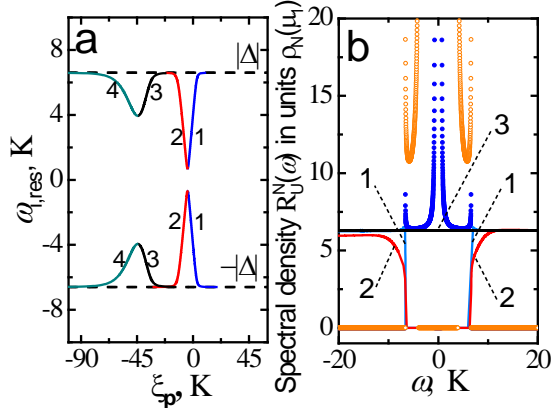
Fig. 4.10 – (a) Spectrum of coherent electron excitations $\omega_{1,res}$ and $\omega_{2,res}$ in a paramagnetic N-metal at $|\Delta| = \Delta_S = 6.6$ K and $\Gamma_S = 0.5$ (curves 1 and 2, respectively) and 5 K (curves 3 and 4, respectively) at frequencies $|\omega_{i\sigma p}| > \Delta_S$; (b) corresponding homogeneous spectral densities of incoherent excitations in the area $|\omega_{i\sigma p}| > \Delta_S$ at $\Gamma_S =$ 0.5 and 5 K (solid curves 1 and 2, respectively) and of coherent excitations from Fig. 4.10a at $\Gamma_S = 0.5$ and 5 K (dark and light points, respectively). The straight line 3 corresponds to the spectral density value 2π in units $\rho_N(\mu_1)$ for an N-metal with a coherent spectrum

The problem considered above corresponds to the simplest case when there is no electron-phonon interaction in the N-metal. Here, it is necessary to take into account an effective field in the N-metal formed by the order parameter $<c_{-p-\sigma}c_{p\sigma}>$ with a corresponding energy gap function

$$\tilde{\Delta}_{k\sigma} = \sum_q \tilde{V}_{k-p}^{el.-ph} <c_{-p-\sigma}c_{p\sigma}>,\qquad(4.46)$$

despite $\tilde{\Delta}_{k\sigma}$ being induced by the effective field of the SC. However, it can be assumed that the induced effective field in the N-metal weakly affects the

self-consistent SC order parameter, especially for highly transparent barriers. Indeed, the induced homogeneous gap function $\Delta_N = \left| \tilde{\Delta}_{k\sigma} \right|$ is represented in the form:

$$\Delta_N = \left| \begin{array}{c} -\dfrac{1}{2}\tilde{\lambda} i \pi \Gamma_S \Delta \times \\[2mm] \displaystyle\int_{-\tilde{\omega}_D}^{\tilde{\omega}_D} d\xi_p \dfrac{1}{\omega_{1\sigma p}-\omega_{2\sigma p}} \left\{ \dfrac{\left[f(\omega_{1\sigma p})-1 \right] sign\left(\arg\left[b(\omega_{1\sigma p}) \right] \right)}{b(\omega_{1\sigma p})} - \dfrac{\left[f(\omega_{2\sigma p})-1 \right] sign\left(\arg\left[b(\omega_{2\sigma p}) \right] \right)}{b(\omega_{2\sigma p})} \right\} \end{array} \right|, \quad (4.47)$$

where $\omega_{1\sigma p}$ and $\omega_{2\sigma p}$ are the roots of Eq. (4.41). Fig. 4.11 shows the dependences of the gap Δ_N on the SC transparency Γ_S at temperature $T = 0$ for various values of Γ_N in the "Al–Sn" hybrid structure where the values $\tilde{\lambda} = 0.175$ and $\tilde{\omega}_D = 423$ K are taken for Al [4.17]. It can be seen that with increasing Γ_S the induced Δ_N increases and then decreases to a value which then weakly depends on electron tunneling. Also, with increasing Γ_N, there is a decrease in Δ_N. Note that the value of the spontaneous gap Δ_S in the absence of tunneling is equal to 6.6 K, $i.\ e.$, significantly exceeds Δ_N.
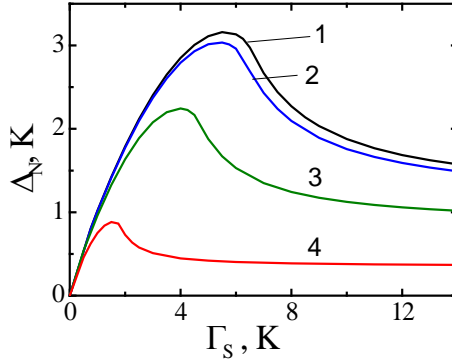
Fig. 4.11 – Gap function Δ_N as a function of the SC transparency Γ_S at the temperature $T = 0$ for different values of the barrier transparencies Γ_N of the N-metal equal to 0.2, 1, 2.5, and 3.4 K (curves 1–4, respectively)

In Fig. 4.12, temperature dependences of the induced in Al gap function with $\Gamma_N = 2.65$ (a) and $\Gamma_N = \Gamma_N^{cr} = 3.495$ K (b) are presented. It can be seen from Fig. 4.12a that with increasing Γ_S the gap Δ_N increases and then decreases in accordance with Fig. 4.11. In this case, only for large transparencies Γ_S a nonmonotonic temperature dependence of Δ_N is observed, and for small Γ_S the

induced gap function decreases monotonically with increasing *T*. Fig. 4.12b shows the temperature dependences of reentrant induced superconductivity at the critical value Γ_N, reflecting a rather complex process of the proximity effect realization in the given hybrid structure.
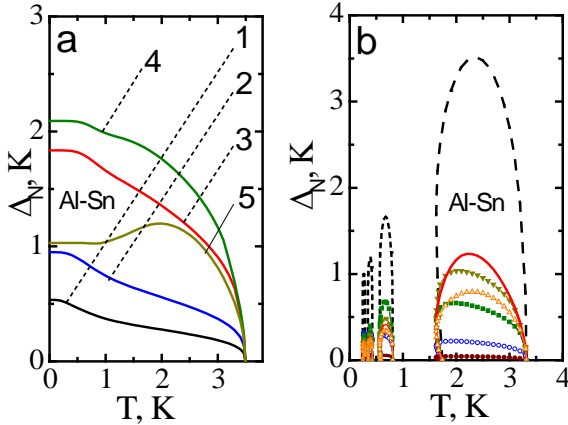
Fig. 4.12 – Temperature dependences of the induced in aluminum gap function Δ_N with $\Gamma_N = 2.65$ (a) and 3.495 K (b) for different barrier transparencies Γ_S of tin: a) 0.5, 1, 2.5, 3.5, and 10 K (curves 1–5, respectively); b) 0.1 (dark points), 0.5 (light points), 1.5 (dark squares), 2.5 (dark triangles), 3.5 (solid line) and 10 K (light triangles). The dotted curve corresponds to spontaneous reentrant superconductivity at the critical transparency $\Gamma_N = 3.495$ in Fig. 4.5
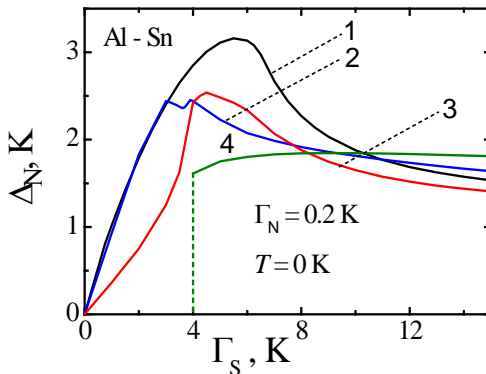
Fig. 4.13 – Induced gap Δ_N as a function of the barrier transparency Γ_S in the ground state for exchange values J_0 equal to 0 (curve 1) and 6 K (curves 2 and 3 at $\sigma = 1, -1$, respectively). Curve 4 corresponds to $J_0 = 10$ K and $\sigma = 1$

At the end, let us study the FM exchange effect on the gap in the N-metal. As mentioned above, the exchange interaction shifts energy bands up and down, depending on the sign of the spin parameter σ, and decreases the gap as well (see Fig. 4.9). Fig. 4.13 shows the gap function Δ_N as a function of the transparency of SC Γ_S at temperature $T = 0$ for various values of the exchange interaction parameter J_0 and spin indices σ equal to 0 (curve 1) and 6 K (curves 2 and 3 at $\sigma = 1, -1$, respectively). It can be seen that at $J_0 < \Delta_S$ in area of the gap maximum for FM the exchange suppresses Δ_N, although for high transparencies the decrease in Δ_N is not so significant. Also, the gaps for the spins $\sigma = 1$ and $\sigma = -1$ differ significantly, that is caused by the asymmetric exchange shift of the electron energy bands with corresponding spins. For $J_0 > \Delta_S$ the difficulties arise in calculating Δ_N at low transparencies Γ_S due to oscillations of the integrand in Eq. (4.47). Therefore, curve 4 at $J_0 = 10$ K in Fig. 4.13 ends abruptly at $\Gamma_S = 4$ K.

4.5 Conclusions

In this chapter, the application of time perturbation theory to a model, in which a self-consistent uniform effective field formed by the electron-phonon coupling of SC induces an order parameter in a N-metal due to electron tunneling, has been considered. Electron-electron scattering has not been taken into account that is true for tunnel areas with linear sizes, which do not exceed an electron mean free path.

It was found that at the critical transparency Γ_N values of the order of the SC critical temperature T_C, tunneling electrons of the N-metal destroy the spontaneous superconductivity in the ground state. The presence of incoherent excitations leads to a complex relationship between the ordering effects, thermal fluctuations, and tunneling, which in the vicinity of $\Gamma_N \sim \Gamma_N^{cr}$ can stabilize the superconducting state in certain temperature ranges. Thus, the phenomenon of the reentrant superconductivity is realized. The study of the direct proximity effect showed that a dimensionless order parameter is induced in the N-metal in the form of an anomalous correlator ,which determines a gap in the spectrum of electron excitations independently of the N-metal effective field.

This field automatically exists when the electron-phonon interaction in this subsystem is taken into account.

The performed numerical calculations for Al showed that the induced energy gap function is significantly smaller than a gap without electron-phonon coupling. It was found that the induced gap first increases and then saturates at high transparency Γ_s values. This means that a further growth in the volume of the superconducting part of the hybrid structure has a small impact on the proximity effect. Also, in the area of the gap Δ_N growth as a function of Γ_s, the FM exchange decreases Δ_N value. The gaps for spin indices $\sigma = 1$ and $\sigma = -1$ differ significantly, that is related to the asymmetric exchange shift of the electron energy bands with corresponding spins. Studied spectral properties of the hybrid structure are in a good agreement with experimental data and also reflect the existence of both coherent and incoherent elementary excitations in certain frequency ranges.

4.6 References to chapter 4

4.1 Kitaev A. Yu. Unpaired Majorana fermions in quantum wires. *Phys.-Usp.* 2001. V. 44. P. s131–s136.

4.2 Gor'kov L. P. On the energy spectrum of superconductors. *Sov. Phys. JETP*. 1958. V. 34. P. 505–508.

4.3 Gennes P. G. Boundary effects in superconductors. *Rev. Mod. Phys.* 1964. V. 36. P. 225–237.

4.4. McMillan W. L. Tunneling model of the superconducting proximity effect. *Phys. Rev.* 1968. V. 175. P. 537–542.

4.5 Eilenberger G. Transformation of Gorkov's equations for type II super-conductors into transport-like. *Z. Phys.* 1968. V. 214. P. 195–213.

4.6 Usadel K. D. Generalized diffusion equation for superconducting alloys. 1970. *Phys. Rev. Lett.* V. 25. P. 507–509.

4.7 Golubov A. A., Kupriyanov M. Yu., Lukichev V. F., Orlikovskiy A. Influence of the proximity effect in the electrodes on the stationary properties of SN-N-NS variable-thickness bridges. *Russ. Microelectron.* 1983. V. 12. P. 355–362.

4.8 Bergeret F. S., Volkov A. F., Efetov K. B. Odd triplet superconductivity and related phenomena in superconductor-ferromagnet structures. *Rev. Mod. Phys.* 2005. V. 77. P. 1321–1373.

4.9 Buzdin A. I. Proximity effects in superconductor-ferromagnet hetero-structures. *Rev. Mod. Phys.* 2005. V. 77. P. 935–975.

4.10 Zdravkov V., Sidorenko A., Obermeier G., Gsell S., Schreck M., Muller C., Horn S., Tidecks R., Tagirov L. R. Reentrant Superconductivity in $Nb/Cu_{1-x}Ni_x$ Bilayers. *Phys. Rev. Lett*. 2006. V. 97. P. 057004.

4.11 Zubov E. E., Zhitlukhina E. S. Effective field approach to transition-metal oxide systems: Magnetism, transport and spectral properties. Vasyl' Stus – DonNU: Vinnytsia, 2019.

4.12 Zubov E. E. Nonlinear proximity effect in a hybrid normal metal-super-conductor structure. *IEEE 10th International Conference Nanomaterials: Applications & Properties*. 2020.

4.13. Mahan G. D. Many particle physics. Plenum: New York. 1990.

4.14. Bardeen J. Handbuch der Physik, Springer-Heidelberg. 1956. V. 15. P. 274.

4.15. Meservey R., Schwartz B. B. Equilibrium properties: comparison of experimental results with prediction of the BCS theory. In "Supercon-ductivity". V. I. Ed. Parks R. D. Marcel Dekker: Inc-New York. 1969.

4.16. Guéron S., Pothier H., Birge N. O., Esteve D., Devoret M. H. Supercon-ductivity proximity effect probed on a mesoscopic length scale. *Phys. Rev. Lett*. 1996. V. 77. P. 3025–3028.

4.17. Gladstone G., Jensen M. A. Schrieffer J. R. Superconductivity in the Transition Metals: Theory and Experiment. In "Superconductivity". V. II. Ed. Parks R. D. Marcel Dekker: Inc-New York. 1969.